Role of positive transfer Q values in fusion cross sections for $^{18}O + ^{182,184,186}W$ reactions

P. Jisha,[1,*] A. M. Vinodkumar,[1] S. Sanila,[1] K. Arjun,[1] B. R. S. Babu,[1] J. Gehlot,[2] S. Nath,[2] N. Madhavan,[2] Rohan Biswas,[2] A. Parihari,[2,†] A. Vinayak,[3] Amritraj Mahato,[4] E. Prasad,[5] and A. C. Visakh[5]

[1]*Department of Physics, University of Calicut, Kerala 673 635, India*
[2]*Nuclear Physics Group, Inter-University Accelerator Centre, Aruna Asaf Ali Marg, New Delhi 110067, India*
[3]*Department of Physics, Karnatak University, Dharwad 580003, India*
[4]*Department of Physics, Central University of Jharkhand, Brambe 835205, India*
[5]*Department of Physics, SPS, Central University of Kerala, Kasaragod 671314, India*

(Received 17 December 2021; revised 14 April 2022; accepted 13 May 2022; published 25 May 2022)

Background: The relevance of including channel coupling effects in the form of target deformation and vibration in fusion reactions has been well established. Many reactions with positive Q values for neutron transfer show enhancement in sub-barrier fusion cross sections. However, there are exceptions to these cases.
Purpose: We aim to make a comprehensive list of factors influencing the sub-barrier fusion enhancement in systems with neutron transfer channels having positive Q values.
Method: Evaporation residue cross sections were measured for $^{18}O + ^{182,184,186}W$ reactions in the energy range 68–104 MeV in the laboratory frame, using a recoil mass spectrometer.
Results: Inclusion of deformation of target and projectile low-level excitations in the coupled channels calculations explains the measured fusion excitation functions of $^{18}O + ^{182,184,186}W$ reactions.
Conclusions: Considering that all the targets have similar deformation, and comparing with $^{16}O + ^{182,184,186}W$ reactions having negative $2n$ transfer Q values, we can conclude that the positive Q values of neutron transfer channels have no effect on the observed fusion cross sections of $^{18}O + ^{182,184,186}W$ reactions.

DOI: 10.1103/PhysRevC.105.054614

I. INTRODUCTION

Nuclear fusion studies are crucial for understanding stellar evolution and power generation in stars. Moreover, investigations into fusion reactions play a vital role in the synthesis of heavy elements and the extension of the periodic table [1–4].

In the collision between two nuclei, a barrier is formed by combining the attractive nuclear potential and the repulsive Coulomb potential. Fusion occurs only when the energy of the incident projectile overcomes this barrier. However, fusion occurs even at energies below the fusion barrier via quantum tunneling, and this has been explained by the one-dimensional barrier penetration model (1D-BPM) [5,6]. In heavy-ion fusion, a significant amount of enhancement was observed in below-barrier fusion cross sections in comparison with 1D-BPM [1,5–8]. Fusion enhancement is affected by the structure of colliding nuclei [9–14] and inclusion of neutron transfer channels [15–21] in the coupled channels (CC) calculations. Incorporating the above mentioned aspects in couplings calculations reduces the fusion barrier and leads to enhanced sub-barrier fusion cross sections; e.g., see Ref. [22].

Barrier distribution (BD) studies also have crucial roles in nuclear reaction and structural studies [23,24]. The BDs are known to be highly sensitive to higher order nuclear deformations. The experimental BDs can be obtained using either fusion cross sections or quasielastic scattering cross sections [25–27]. The heights of the barriers in the barrier distributions can be reduced by inclusion of transfer channels in CC calculations, even with a low transfer strength. Transfer strength is usually determined from measured transfer angular distributions. Existing theoretical models [28–30] have already identified the role of nuclear deformation and vibration in the enhancement of experimental sub-barrier fusion cross sections. However, further understanding of the role of neutron transfer channels in fusion enhancement is required.

The effect of the positive Q value of the neutron transfer (PQNT) on the sub-barrier fusion enhancement was first observed by Beckerman *et al.* [31] in the $^{58}Ni + ^{64}Ni$ system. Broglia *et al.* [20,32] further theoretically explained such an enhancement due to positive Q value transfer channels. Studies on $^{40}Ca + ^{44,48}Ca$ added evidence for the fusion enhancement in below-barrier fusion cross sections due to PQNT [33]. Theoretical studies of Stelson [34] proposed that neutron transfer may start at distances far away from the barrier distance itself, which creates a neck between the colliding nuclei. This neck formation reduces the barrier and causes fusion enhancement. Several experimental studies attributed the enhancement in fusion cross sections to the PQNT channel [16,18,19]. Experimental studies on systems like $^{32}Si + ^{100}Mo$ [35], $^{40}Ca + ^{90,96}Zr$ [27,36], $^{32}Si + ^{110}Pd$ [37], $^{40}Ca + ^{124,132}Sn$ [18], $^{40}Ca + ^{70}Zn$ [38], etc. confirmed the PQNT channel effects. However, many measurements, such as those from $^{18}O + ^{118}Sn$ [39], $^{17}O + ^{144}Sm$

*jisha_dop@uoc.ac.in
†Presently at Department of Physics and Astrophysics, University of Delhi, New Delhi 110007, India.

[9], ^{58,64}Ni + ^{130}Te [40], ^{58,64}Ni + ^{132}Sn [40], ^{60,64}Ni + ^{100}Mo [41], ^{16,18}O + ^{76,74}Ge [42], etc., do not show a significant fusion enhancement in the below-barrier energy region even with a PQNT channel.

The inclusion of PQNT in CC calculations explained the fusion enhancement in many cases; however, its presence alone is not sufficient to explain the enhanced cross sections. The goal of many of the systematics and theoretical studies was to figure out what was causing the fusion enhancement. To find the influence of neutron transfer on the fusion excitation function, Jiang *et al.* [43] carried out a systematic study, and their results show that significant enhancement was possible in systems with neutron-poor projectiles and neutron-rich targets. Rachkov *et al.* [44] pointed out that the PQNT channel significantly influences sub-barrier fusion when the system has large positive Q values for neutron transfer and the coupling to the collective states is weak at sub-barrier energy. Further, the systematic investigations of Zhang *et al.* [45] on systems with PQNT observed that. after neutron transfer, fusion enhancement occurs when the deformation of interacting nuclei increases and the mass asymmetry of the system decreases. The deformation of nuclei having a similar effect on transfer coupling can be seen elsewhere [46–48].

The relevance of neutron transfer with positive Q values for nuclear fusion lies in the insensitive nature of the Coulomb barrier to the neutrons. For radioactive and weakly bound nuclei, couplings to neutron transfer play a significant role in enhancing fusion at below-barrier energies. Such a large influence of neutron transfer is most likely due to the extended wave functions of the loosely bound neutrons [17,49]. Studies on weakly bound nuclei showed that the coupling to breakup channels enhances cross sections for complete fusion at energies below the Coulomb barrier, while it reduces them at energies above [50,51]. However, determining the involvement of weakly bound nucleons in sub-barrier fusion is difficult due to the difficulty of simultaneously considering decay channels as well as nucleon transfer in complete fusion [49,52].

Even with several theoretical works [28,29,34,53,54] in the area of transfer and fusion, a detailed understanding of PQNT on sub-barrier fusion is missing [55]. This lack of a comprehensive idea about transfer is due to the difficulties in integrating these channels into theoretical models. There is not sufficient experimental data to get a clear understanding of this aspect.

In the present work, for evaporation residue measurements we have selected ^{18}O + ^{182,184,186}W reactions, which have a positive Q value for $2n$ transfer. The goal of this study is to compare the fusion cross sections of these reactions to those of ^{16}O + ^{182,184,186}W reactions [56–58], which have negative Q value for $2n$ transfer. Even though the compound nuclei (CN) formed in ^{18}O + ^{182,184,186}W reactions are fissile, the fission cross section in the below-barrier energy region is negligible. Thus, there will be no undesired bias when comparing the fusion cross sections of ^{16}O + ^{182,184,186}W with evaporation residue (ER) excitation functions of ^{18}O + ^{182,184,186}W in the below-barrier energy regions. In the case of ^{18}O induced reactions after $2n$ transfer, the target-like nuclei show a change in deformation. Also, different observations by Rachkov *et al.* [44] showed that, for colliding nuclei with a magic proton or neutron number, neutron rearrangement would play a significant role in fusion enhancement.

Even with a high positive transfer Q value, fusion excitation functions of ^{18}O on different isotopes of Sn do not show enhancement in the sub-barrier energy range [47,48,59]. However, recent work of Deb *et al.* [60] shows an increase in the below-barrier fusion cross sections for ^{18}O + ^{116}Sn due to the PQNT effects. Like Sn isotopes, ^{182,184,186}W, which exhibit a more significant deformation, will be an ideal selection to study the role of the PQNT channel on fusion enhancement in the heavy mass region. The majority of ^{18}O induced reactions have negative Q_{1n} transfer and positive Q_{2n} transfer, which prevents a sequential transfer and favors a pair transfer. Esbensen *et al.* [33] attributed a strong pair-transfer channel with a positive Q value to fusion enhancement in below-barrier cross sections. Due to the rarity of ^{18}O-induced reactions in heavy-ion fusion, ^{18}O + ^{182,184,186}W will be a good candidate for studying the neutron transfer effect in heavy-ion fusion enhancement in the below-barrier energy regions.

The present work is organized as follows. Section II discusses the experimental setup and technique, followed by Sec. III, which details the analyses done. Section IV contains descriptions of coupled channels calculations, as well as comparisons of these calculations with experimental data. Section V has a summary and conclusion.

II. EXPERIMENTAL DETAILS

The experiment was performed at the 15 UD Pelletron accelerator facility of the Inter-University Accelerator Centre (IUAC), New Delhi. The experiment was carried out using Heavy Ion Reaction Analyser (HIRA) [61], which was kept at zero degrees to the beam direction with a 10 msr entrance aperture. A pulsed beam of ^{18}O with 4 μs pulse separation bombarded the isotopically enriched targets of ^{182}W (91.6%), ^{184}W (95.2%), and ^{186}W (94%) with approximate thicknesses of 70, 300, and 100 μg/cm^2 respectively. ER excitation functions were measured at laboratory beam energies of 68 to 104 MeV (10% below to 35% above the fusion barrier) in 2–4 MeV energy steps.

Two silicon surface barrier detectors (SSBDs) of active area 50 mm^2 each with a collimator diameter of 1 mm were placed at a distance of 90 mm from the target inside the target chamber. The SSBDs were placed at angles of $\pm$ 15° to beam direction for normalization of ER cross sections. A carbon foil with a thickness of 40 μg/cm^2 was placed 10 cm downstream from the target for equilibration of the charge states of ERs. A multiwire proportional counter (MWPC) of active area 150 × 50 mm^2 was placed at the focal plane (FP) of HIRA to detect the ERs. A time of flight (ToF) was set up between the anode signal of the MWPC and the rf signal to separate the scattered beam-like particles from ERs. Data acquisition was carried out using a computer automated measurement and control (CAMAC) based system, and analysis was performed with the software CANDLE [62].

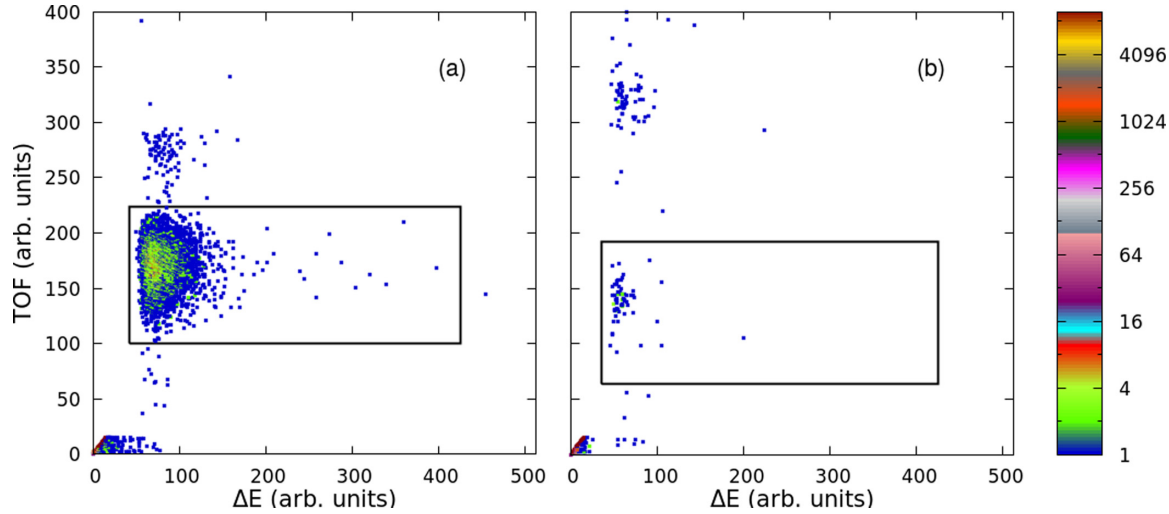

FIG. 1. Scatter plot between ΔE and ToF of the events recorded at the focal plane of HIRA for the $^{18}\mathrm{O}+{}^{186}\mathrm{W}$ reaction at energies (E_{lab}) 80.0 and 70.0 MeV are shown in panels (a) and (b) respectively.

III. DATA ANALYSIS

The total ER cross section was calculated using the equation

$$\sigma_{\mathrm{ER}} = \frac{Y_{\mathrm{ER}}}{Y_{\mathrm{norm}}}\left(\frac{d\sigma}{d\Omega}\right)_{\mathrm{Ruth}} \Omega_{\mathrm{norm}}\left(\frac{1}{\epsilon_{\mathrm{HIRA}}}\right), \tag{1}$$

where Y_{ER} is the number of ERs detected at the FP of the HIRA, Y_{norm} is the number of elastically scattered projectile-like particles detected by the normalization detectors, $(\frac{d\sigma}{d\Omega})_{\mathrm{Ruth}}$ is the differential Rutherford-scattering cross section in the laboratory system, Ω_{norm} is the solid angle subtended by the normalization detectors, and ϵ_{HIRA} is the average ER transmission efficiency of HIRA. There were two significant challenges in the extraction of σ_{ER} from the experimental data. One was the estimation of ϵ_{HIRA}, the efficiency of the spectrometer, and the other was the unambiguous recognition of ERs at the HIRA focal plane.

ϵ_{HIRA} is a dynamic function of many parameters that are unique to the reaction and the instrument. Transmission efficiency ϵ_{HIRA} is the ratio of the number of ERs reaching the focal plane of HIRA to the total number of ERs emerging out of the target for a reaction under consideration. It is a function of parameters such as the beam energy, entrance-channel mass asymmetry, target thickness, magnetic field, angular acceptance of the separator, and the exit channels of interest. Since it was not practical to find the efficiency of each exit channel separately, we relied on a Monte Carlo code, TERS [63,64], to find channel-wise efficiency. We calculated the efficiency for all channels (which contribute more than ≈1% of total ER cross section) using TERS and estimated ϵ_{HIRA} for each energy by taking the weighted average of all efficiencies over total ER. The relative population of each channel for calculating the weighted average was estimated using statistical model code PACE4 [65]. These average HIRA efficiency values generally have ≈10% uncertainty.

Another matter of considerable importance was the unambiguous identification of ER at the FP detector. The ER identification was achieved by simultaneously measuring energy loss, ΔE (measured at the cathode of the MWPC), and ToF of the ERs, providing a clear separation of ERs from projectile-like background events. The scatter plots of ΔE versus ToF at $E_{\mathrm{lab}} = 80.0$ and 70 MeV for the reaction $^{18}\mathrm{O}+{}^{186}\mathrm{W}$ are shown in Fig. 1. The relative strength of background events on the HIRA FP detector, although negligible in most cases, was observed to increase gradually with a decrease in E_{lab} for below-barrier energies [66]. In the present investigations, we obtained adequate distinction between ERs and background events across the entire range of E_{lab}. The measured ER cross sections as a function of projectile energies in the center-of-mass frame ($E_{c.m.}$) and laboratory frame (E_{lab}) are listed in Table I. The sum of statistical and systematic errors is quoted as the total error in the measurement. The overall error was estimated to be $\leqslant$ 20% below the barrier energies. In the total error, the major part is from ϵ_{HIRA} (≈10%). Statistical model calculations [65] of $^{18}\mathrm{O}+{}^{182,184,186}\mathrm{W}$ revealed that the calculated fission cross sections are negligibly small in the measured energy range. For $^{18}\mathrm{O}+{}^{182,184,186}\mathrm{W}$ reactions, the estimated fission cross sections are 5%, 3%, and 2% respectively at the highest energies where measurements were carried out. Hence, ER cross sections in the energy range of measurements were considered as σ_{fus} in the present study.

IV. RESULTS AND DISCUSSION

Coupled channels calculations [28,29] explain the fusion cross section rather well at lower excitation energies by precisely considering different degrees of freedom such as deformation of colliding nuclei, collective surface vibrations, and neutron transfer. In the present study, CC calculations were carried out to explore the effect of coupling of different states of the targets and projectile below the Coulomb barrier energy region.

TABLE I. Measured ER cross sections for ^{18}O+^{182,184,186}W reactions. The quoted errors include systematic and statistical errors.

^{18}O+^{182}W			^{18}O+^{184}W			^{18}O+^{186}W		
E_{lab} (MeV)	$E_{c.m.}$ (MeV)	σ_{ER} (mb)	E_{lab} (MeV)	$E_{c.m.}$ (MeV)	σ_{ER} (mb)	E_{lab} (MeV)	$E_{c.m.}$ (MeV)	σ_{ER} (mb)
104.0	94.52	1081 ± 152	104.0	94.43	766 ± 134	104.0	94.67	767 ± 91
100.0	90.87	1094 ± 151	100.0	90.78	887 ± 171	100.0	91.02	673 ± 78
96.0	87.23	786 ± 285	96.0	87.12	932 ± 195	96.0	87.37	723 ± 87
92.0	83.58	778 ± 130	92.0	83.48	815 ± 168	92.0	83.72	656 ± 77
88.0	79.94	590 ± 81	88.0	79.83	705 ± 129	88.0	80.07	606 ± 71
84.0	76.30	368 ± 59	84.0	76.17	369 ± 69	84.0	76.41	484 ± 54
80.0	72.65	194 ± 35	80.0	72.52	182 ± 30	80.0	72.76	215 ± 25
78.0	70.83	120 ± 24	78.0	70.69	129 ± 22	78.0	70.93	164 ± 18
76.0	69.01	55.4 ± 7.9	76.0	68.87	68.5 ± 11.2	76.0	69.11	73.4 ± 8.7
74.0	67.19	26.3 ± 3.8	74.0	67.04	32.3 ± 3.9	74.0	67.28	24.5 ± 3.0
72.0	65.37	9.03 ± 1.40	72.0	65.22	7.17 ± 1.45	72.0	65.46	8.61 ± 1.25
70.0	63.55	1.53 ± 0.25	70.0	63.38	2.55 ± 0.53	70.0	63.63	1.11 ± 0.21
68.0	61.73	0.24 ± 0.05	68.0	61.80	0.31 ± 0.06			

A. Coupled channels calculation

The fission cross sections for ^{18}O + ^{182,184,186}W reactions are negligibly small in the below-barrier energy regions. Hence, we can directly compare the measurements against the coupled channels calculations. The measured fusion cross sections for ^{18}O + ^{182,184,186}W reactions are analyzed using coupled channels code CCFULL [28,29,67]. The cross sections are first compared with the 1D-BPM calculations. Contributions of inelastic states of colliding nuclei are also included in the computations to study the channel coupling effects. Table II lists the projectile and target excitation energies and their corresponding deformations.

The Akyuz-Winther (AW) parametrization of nuclear potential is used to obtain Woods-Saxon potential parameters in CC calculations. For CC calculations, parameters such as depth of potential (V_0), radius (r_0), and diffuseness (a), are taken from the closest system, ^{16,18}O + ^{181}Ta [72]. The parameters V_0, r_0, and a are selected as 98.76 MeV, 1.15 fm, and 0.73 fm for CC calculations, which reproduces the experimental fusion barriers for ^{16}O + ^{182,184,186}W reactions. The cross sections from CCFULL calculations with these potential parameters without including any coupling are termed 1D-BPM excitation functions. For ^{16}O + ^{182,184,186}W reactions, 1D-BPM calculations explain the fusion cross sections in the above-barrier region.

In order to explain the below-barrier fusion cross sections of ^{16}O + ^{182,184,186}W reactions, first we include the lowest energy state (that is, the 3^- state) of ^{16}O having energy 6.130 MeV and octopole deformation $\beta_3 = 0.729$ [73] in the CC calculations. The inclusion of the 3^- state of ^{16}O alone in CC calculations shows higher values compared to the experimental fusion cross section, as shown by brown dotted lines in Figs. 2(a), 2(b), and 2(c). According to Hagino *et al.* [74], the energy of the 3^- state of ^{16}O is very high compared to the curvature ($\hbar\omega$) of the excitation function and its inclusion in the CC calculations will have a re-normalization effect on the static potential without significantly changing the shape of the barrier distribution. In the same way, inclusion of the 3^- state in CC calculations of ^{16}O + ^{182,184,186}W reactions gives higher theoretical values compared to the experimental fusion data. Accordingly, corresponding coupling was not included in our final CC calculations. We treat the ^{16}O as spherical for CC calculations of ^{16}O + ^{182,184,186}W reactions. Also, we treat the tungsten isotopes as deformed. In CC calculations we included their 0.250, 0.234, 0.226 quadrupole and −0.066, −0.093, −0.045 hexadecapole deformations respectively for ^{182,184,186}W nuclei. Thus, coupling of quadrupole and hexadecapole deformation of the target with the relative motion of colliding nuclei explained the fusion cross sections of ^{16}O + ^{182,184,186}W, as shown by the brown solid lines in Figs. 2(a), 2(b), and 2(c).

The same set of deformation parameters used for the target nuclei in ^{16}O + ^{182,184,186}W reactions are used for the CCFULL calculations of ^{18}O + ^{182,184,186}W reactions also. Eventually projectile excitations are added in the CC calculations. With the inclusion of the 3^- state of ^{18}O with energy 5.097 MeV [73] and octopole deformation 0.595 [75] along with the quadrupole and hexadecapole deformation of targets, CC calculations show higher cross sections as compared to the experiment, as shown by the brown dotted lines in Figs. 3(a), 3(b), and 3(c). Thus the 3^-, state of ^{18}O is not included in the final CC calculations. We observe that the 2^+ vibrational state of ^{18}O with energy 1.982 MeV coupled with the quadrupole and hexadecapole deformations of ^{182,184,186}W reproduce the experimental cross sections of ^{18}O + ^{182,184,186}W reasonably in the whole energy range. The calculated results, which reproduce the experimental cross sections of ^{18}O + ^{182,184,186}W

TABLE II. Deformation parameters and first excitation energies of different nuclei used in the CC calculations.

Nucleus	Energy of first excited state (MeV)	β_2	β_4	Ref.
^{16}O(Sphe.)				
^{18}O(Vib.)	1.982	0.355		[68]
^{182}W(Rot.)	0.100	0.251	−0.066	[68,69]
^{184}W(Rot.)	0.111	0.236	−0.093	[68,69]
^{186}W(Rot.)	0.122	0.226	−0.045	[68,70]

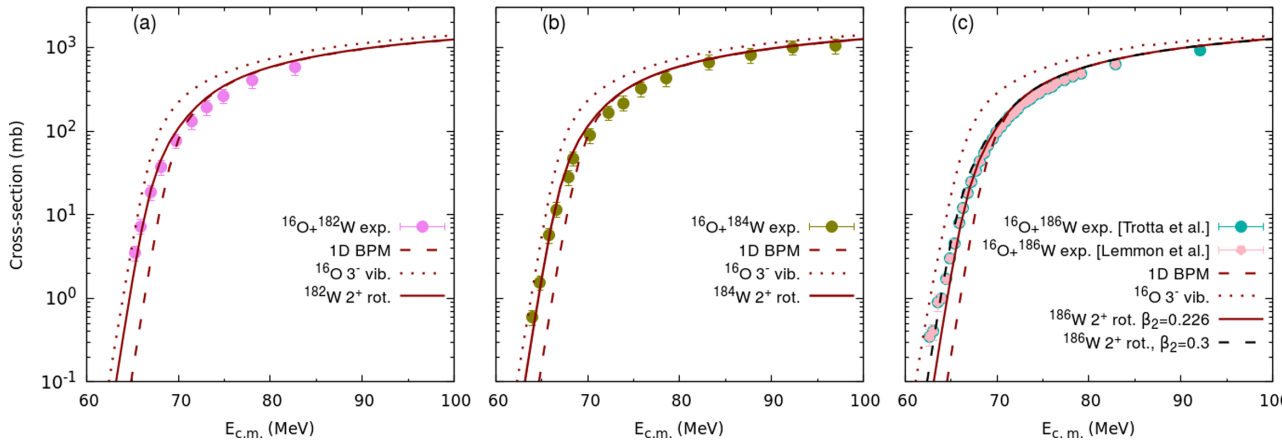

FIG. 2. Fusion excitation functions for the ^{16}O + ^{182,184,186}W reactions. The violet, olive-green, and cyan solid circles are experimental cross sections of ^{16}O + ^{182,184,186}W reactions from Refs. [57,58,70,71] respectively. The dashed lines represent the CC calculations without any coupling (1D-BPM). The solid and dotted lines represents theoretical fusion cross sections obtained after including the deformation of targets and vibrational state of projectile respectively in CC calculations. Black dashed lines in panel (c) represents CC calculations of ^{16}O +^{186}W after including the deformation of the target with a modified quadrupole deformation parameter $\beta_2 = 0.3$.

reactions, are shown by brown solid lines in Figs. 3(a), 3(b), and 3(c).

In the below-barrier energy regions, to explain the enhanced fusion cross sections, Esbensen *et al.* [33] considered the presence of a strong pair-transfer channel with a positive Q value. All ^{18}O induced reactions under this study possess a positive $2n$ transfer channel. Thus, $2n$ transfer channels are included in the coupling scheme of ^{18}O +^{182,184,186}W reactions to see the effect of the PQNT channel on below-barrier fusion cross sections. ^{18}O +^{182,184,186}W reactions have positive Q values of 1.414, 0.757, 0.133 MeV respectively for the $2n$ stripping channel. The CCFULL code [28,29] has an option to include one transfer channel in the calculations. It can be a proton or neutron channel. The calculations are done including both the $2n$ transfer channel and the inelastic excitations. The result is illustrated as green double-dotted dashed lines in Figs. 3(a), 3(b), and 3(c). The neutron transfer coupling has been included in the CCFULL code for the present system through the transfer coupling strength parameter for $2n$ transfer.

The code CCFULL accounts for the transfer channel through the macroscopic transfer coupling form factor, F_{tr}(r). In principle, the form factor is estimated from the differential and total transfer cross sections [76,77] as mentioned in the Introduction. Since experimental transfer measurements do not exist for this system, the transfer form factor is unknown, and only a qualitative measure of the transfer strength is possible. The coupling strength is related to the form factor by the relation $F_{tr}(r) = F_{tr}\frac{dV_N}{dR}$. The coupling strength in the CCFULL calculations was varied until a fairly good agreement with experimental data was achieved, as done by Deb *et al.* [60]. The green double-dotted dashed lines in Figs. 3(a), 3(b), and 3(c) shows results of CCFULL calculations after including a transfer channel with a transfer strength 0.42 fm along with

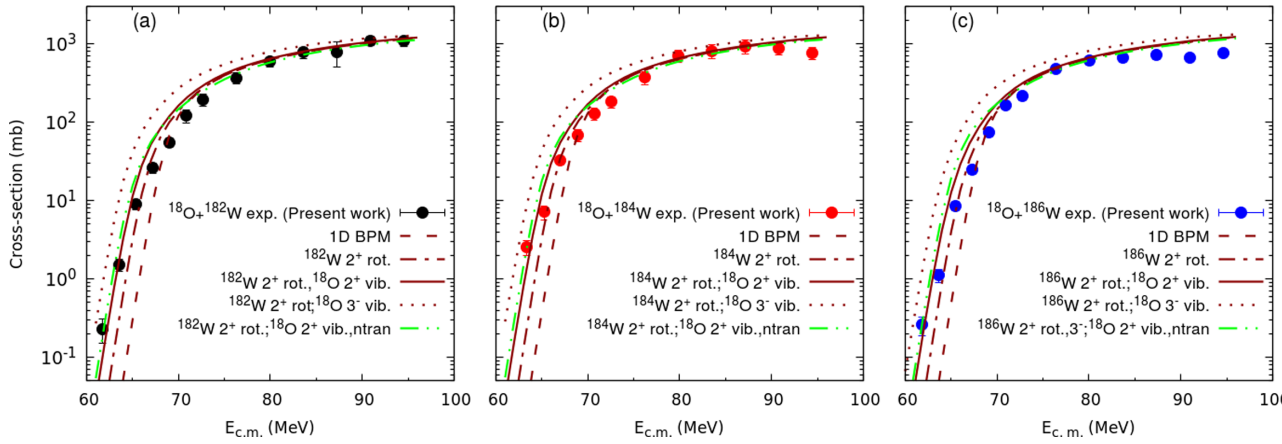

FIG. 3. Fusion excitation functions for ^{18}O + ^{182,184,186}W reactions. The black, red, and blue solid circles are experimental results. The dashed lines represent the CC calculations without any coupling (1D-BPM). The solid lines represent CC calculations with 2^+ vibrational state of projectile and deformation of targets. Dotted lines represent CC calculations with 3^- vibrational state of projectile and deformation of targets. Green double-dotted dashed lines represents CC calculations after including neutron transfer.

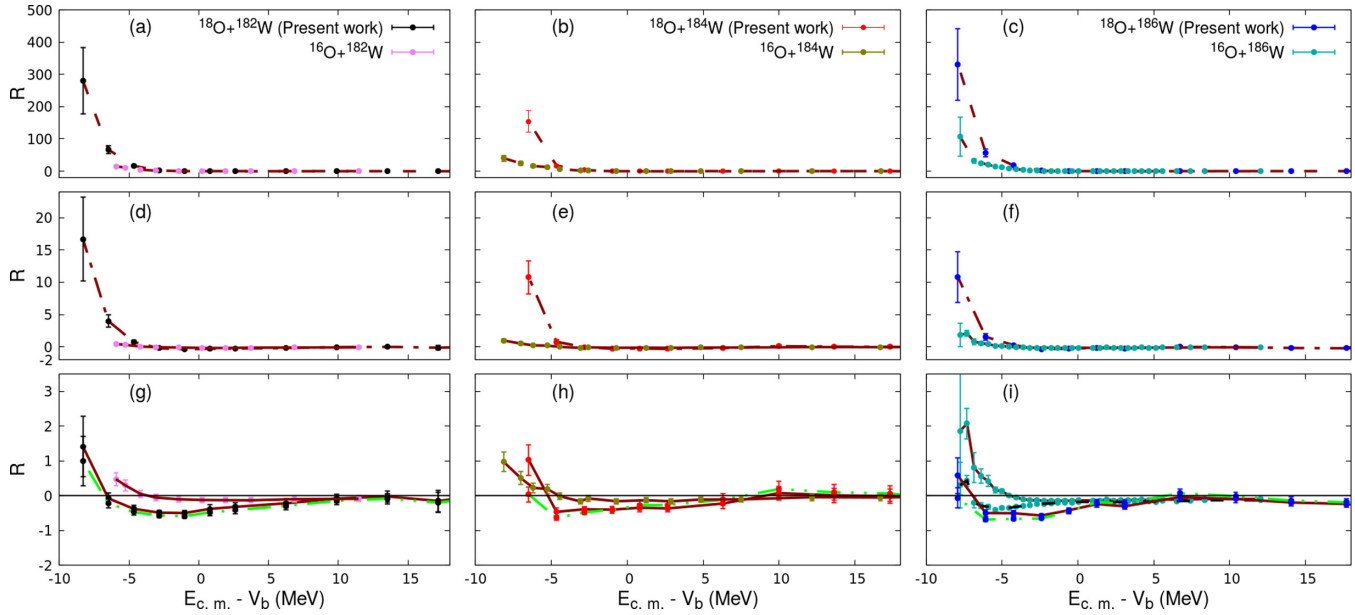

FIG. 4. Relative change as a function of $E_{c.m.} - V_b$ for ^{16,18}O + ^{182,184,186}W. Panels (a), (b), and (c) represent relative change in experimental cross sections from 1D-BPM. Panels (d), (e), and (f) represent the relative change of experimental cross sections from the CC calculations after including target rotations. Plots for ^{18}O + ^{182,184,186}W in panels (g), (h), and (i) represent R after including 2^+ vibrational state of projectile and deformations of targets in CC calculations. For ^{16}O induced reactions, the same figures include deformation of targets only. Black, red, and blue solid circles connected by green double-dotted dashed lines represent R after including neutron transfer. Cyan solid circles connected by black dashed lines in panel (i) represent R of ^{16}O + ^{186}W with a modified deformation $\beta_2 = 0.3$ in CC calculations.

inelastic excitations. Beyond a coupling strength of 0.5 fm, CC calculations started deviating from the experimental measurements. It is difficult to distinguish or separate the theoretical excitation function with neutron transfer from that without transfer channels. Thus, without invoking the coupling of the transfer channel, which was one of the motivations for the measurement, CC calculations explained experimental data.

B. A self-consistent method: Relative change

We define the term relative change (R) to provide better predictions about the effects of neutron transfer channels on fusion reactions of ^{18}O + ^{182,184,186}W. The positive or negative values of R respectively quantify the increase or decrease in experimental cross sections as compared to theoretical ones. R is defined as the ratio of the difference between the experimental (σ_{exp}) and theoretical (σ_{theo}) fusion cross sections to the theoretical fusion cross section, i.e., $R = (\sigma_{exp} - \sigma_{theo})/\sigma_{theo}$. We quantify R by incorporating several possible inelastic excitations together with the relative motion in the CC calculations. After incorporating inelastic channels in CC calculations, R is expected to be zero for ^{16}O + ^{182,184,186}W reactions, where the PQNT effect was not expected. Accordingly, these reactions are taken as the benchmark for comparing the enhancement due to PQNT in ^{18}O + ^{182,184,186}W reactions.

First, we calculate the values of R in ^{16}O and ^{18}O induced reactions using only 1D-BPM. All six reactions exhibit a value for R greater than zero at energies below the Coulomb barrier. Since R indicates the relative increase in experimental cross sections with respect to the theory, any values of R greater than zero imply lower cross section values of the theory. Also, increase in R indicates the absence of inelastic channels in the coupling. Accordingly, to account for the experimentally observed cross sections, it is necessary to include inelastic channels in the coupling at below-barrier energies. Which is shown by solid circles connected by brown dashed lines in Figs. 4(a), 4(b), and 4(c). R of ^{18}O induced reactions has larger values than that of ^{16}O induced ones at below-barrier energies. The enhancement effect compared to 1D-BPM calculations is higher in ^{18}O + ^{184,186}W reactions than ^{16}O induced ones. This may be an indication that more channels should be added in the coupling calculations of ^{18}O to reproduce the experimental values compared to ^{16}O induced reactions. In the case of the ^{16}O + ^{182}W reaction, cross sections for the lower energies are not available [56]. Due to this it will be difficult to make comparative statements regarding larger R values compared to 1D-BPM calculations in the ^{18}O + ^{182}W reaction than in the ^{16}O + ^{182}W reaction. After including the quadrupole and hexadecapole deformations of the target, ^{18}O induced reactions show R greater than zero, which maximizes at sub-barrier energy regions as shown in Figs. 4(d), 4(e), and 4(f). Therefore it is necessary to include an additional coupling to explain below-barrier cross sections. Here the additional coupling is the vibrational excitations of the ^{18}O projectile. For ^{16}O induced reactions, R approaches zero for most of the below-barrier energy points while including deformation of targets in CC calculations. This zero R value indicates a good agreement between theory and experiment. The theoretical compliance is shown by solid circles connected by brown colored solid lines in Figs. 4(d), 4(e), and 4(f). Among different possible coupling channels, we have considered only the deformation of

the targets for ^{16}O induced reactions. After that, R approaches zero for all energy points and shows a slight deviation only at one energy point in the sub-barrier energy region. For ^{18}O induced reactions, we have to include the vibrational coupling of the projectile in addition to quadrupole and hexadecapole deformation of the targets to explain the deviation of R from zero. After including vibrational excitation of the projectile and deformation of the target in the coupling, the theoretical excitation function agrees well with the experimental data for all ^{18}O induced reactions in below-barrier energy regions. It is shown as black, red, and blue solid circles connected by the brown colored solid lines in Figs. 4(g), 4(h), and 4(i).

To explore the effect of PQNT channels in fusion cross sections, we have calculated R including the neutron transfer channel in ^{18}O + ^{182,184,186}W reactions. Even the addition of a neutron transfer channel in coupling does not improve the agreement between the experiment and theory. This indicates that, contrary to expectations, coupling of the neutron transfer channel in CC calculations does not provide any robust increase to the theoretical cross sections of ^{18}O + $^{182+,184,186}$W. Solid circles connected by green double-dot dashed lines in Figs. 4(g), 4(h), and 4(i) show R obtained for ^{18}O + ^{182,184,186}W reactions after including neutron transfer channels. As seen in Figs. 4(g), 4(h), and 4(i), R with neutron channel does not deviate significantly from that without neutron transfer channel inclusion. The $2n$ transfer Q values of (^{18}O + ^{182}W) > (^{18}O + ^{184}W) > (^{18}O + ^{186}W). However, increase in cross sections with the increase in $2n$ transfer Q value is not observed at the below-barrier energy levels of these reactions.

At below-barrier energies, CC calculations of ^{16}O + ^{186}W show lower values compared to the experimental cross sections. R shows a bit higher value, beyond $E_{c.m.} - V_b = -7$ MeV. For the ^{16}O + ^{186}W reaction, many works [56,57,70,78] explained the enhanced below-barrier cross sections. Among these the ANU group [56,57,70] used potential parameters, and diffuseness deduced from elastic scattering data for CC calculations. The associated deformation parameters of ^{186}W were $\beta_2 \approx 0.24$ and $\beta_4 \approx -0.09$. They also tried to fit the fusion data of ^{16}O + ^{186}W by varying potential parameters and deformation. They obtained an optimum fit with a diffuseness $a = 1.27$ fm and with an average barrier of 68.9 MeV, and also obtained best-fit deformation parameters $\beta_2 \approx 0.3$ and $\beta_4 \approx -0.045$. This β_2 value is larger than that obtained from elastic scattering data, and β_4 was smaller than that of non-fusion data observed by Lemmon *et al.* [70]. The possible explanation for this lies in the change in the shape of the barrier distribution. Generally, any additional coupling effects will result in the smoothing of the barrier. However, the effect of coupling will have a higher impact when the barrier distribution has sharp changes. Effect of deformations will be predominant in such systems [70]. The barrier distribution of the ^{16}O + ^{186}W reaction shows a sharp change before adding the coupling [70]. We have carried out the CC calculations for the ^{16}O + ^{186}W reaction with deformation parameters $\beta_2 \approx 0.3$ and $\beta_4 \approx -0.045$, which were used by Lemmon *et al.* [70] to explain the fusion data. The corresponding results are shown as a black dashed line in Fig. 2(c). Calculations with deformation values extracted from elastic scattering data are also shown in Fig. 2(c) as a brown solid line. R calculated with this modified deformation value is shown as solid circle connected by black dashed lines in Fig. 4(i). Figure 4(i) shows that the deviations of R from zero vanishes at below-barrier energy points with this modified deformation value and shows good agreement between the theory and the experiment.

Excitation functions of ^{16}O + ^{182,184,186}W systems, which all have negative transfer Q value for neutron transfer, are explored using coupled channels calculations. The coupling of relative motion of colliding partners with inelastic excitations of target was enough to explain the experimental cross sections above and below the Coulomb barrier energy regions as shown in Figs. 2 and 4. In the measured energy range, the 2^+ vibrational state of ^{18}O coupled with the quadrupole and hexadecapole state of ^{182,184,186}W show a relatively good agreement between the calculated and experimental results. An additional coupling of neutron transfer channel in ^{18}O + ^{182,184,186}W reactions do not show a different R value from calculations without neutron transfer. Plots in Figs. 4(g), 4(h), and 4(i) with solid circles joined by green double dotted dashed lines shows R with neutron transfer channel.

The Q values for the $2n$ transfer processes are positive for all reactions with ^{18}O. Thus, the neutron transfer can be important for the reactions with the ^{18}O beam. However, our results show that cross sections for reactions with ^{16}O and ^{18}O induced reactions are very similar. A small decrease in deformation of the target after $2n$ transfer may explain this results. Coulomb barriers of the systems before and after $2n$ transfer are almost the same, and, correspondingly, their fusion cross sections are similar [47,48]. Such results are observed in many systems like ^{16,18}O + ^{76,74}Ge [80–82], ^{16,18}O + ^{112,118,124}Sn [39], etc.

C. Systematics of ^{18}O induced reactions

A positive $2n$ transfer Q value characterizes the majority of ^{18}O induced reactions. Several experiments in low, medium, and heavy mass regions have been carried out to investigate the effect of the $2n$ transfer Q value in fusion cross sections induced by ^{18}O [42,59,60,72]. Compared to other transfer channels, $2n$ transfer has a significant effect on sub-barrier fusion enhancement [38]. Montagnoli and Stefanini [8] suggested that, when heavier systems are compared, multiphonon excitations have a more significant impact on sub-barrier fusion. Also, if multiphonon excitations are dominant, then the effect of PQNT will be weaker in the case of heavier systems [8]. Thus, the effect of PQNT channels can only be seen at extremely low energies. To make conclusive remarks on the effect of PQNT on heavier systems, a systematic study in the same mass regions is needed.

For a systematic study in the heavy mass region, we compared the reduced fusion cross sections of several ^{18}O induced reactions with those of ^{16}O induced ones (having negative neutron transfer Q value). Reduced cross section will eliminate the effects of the barrier height and nuclear size [51]. We eliminated the effects of geometrical aspects by using traditional reduction methods ($\tilde{\sigma}_{fus} = \frac{\sigma_{fus}}{\pi R_b^2}$, where R_b the barrier radius). When compared to ^{16}O induced reactions in the heavy

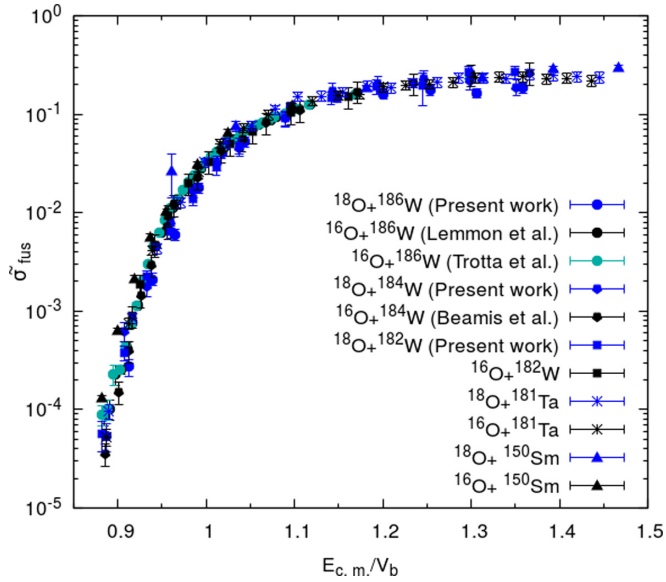

FIG. 5. Reduced fusion cross sections as a function of $E_{c.m.}/V_b$ for reactions induced by ^{16,18}O. Here, the reduced cross section is obtained by dividing absolute cross section with πR_b^2, where V_b and R_b are the Bass barrier and Bass radius [75]. The fusion cross sections of $^{16,18}O+^{150}Sm$ [79], $^{16,18}O+^{181}Ta$ [72], $^{16}O+^{182}W$ [58], $^{16}O+^{184}W$ [71], and $^{16}O+^{186}W$ [57,70] are obtained from literature.

mass region as seen in Fig. 5, ^{18}O induced reactions do not exhibit a significant increase. In the majority of the systems under investigation, there is no discernible enhancement in below-barrier fusion cross sections. The $^{18}O+^{150}Sm$ system is the only one that shows enhancement in the below-barrier region when compared to the ^{16}O induced reference system. The reduced cross section of $^{18}O+^{181}Ta$ does not exhibit fusion enhancement in the below-barrier region, compared to the reference system $^{16}O+^{181}Ta$ as seen in Fig. 5. When compared to reference systems, there is no noticeable enhancement in $^{18}O+^{182,184,186}W$ reactions as seen in Fig. 5. Our CC calculations on the same reactions, discussed in Sec. IV A, also conclude the same. The deviating behavior of $^{18}O+^{150}Sm$ may be attributed to the change in the deformation of the target nuclei after $2n$ transfer. All other reactions that we considered in our study show a decrease in deformation of the target nuclei after $2n$ transfer, whereas $^{18}O+^{150}Sm$ shows an increase. Examining the deformation values of the target nuclei in $^{18}O+^{150}Sm$ reactions revealed a relatively higher change in deformation after neutron transfer when compared to other systems. The present measurements, as shown in Fig. 5, exhibit a spread in excitation function in the above-barrier energy regions. It could be attributed to the presence of other channels such as noncompound nuclear fission or breakup channels, etc. [1].

To check whether the reason for enhancement in $^{18}O+^{150}Sm$ is extendable to low and medium mass regions, we have carried out a systematic study on all ^{18}O induced reactions available in the literature. Table III lists the reactions used in the systematic study as well as their transfer Q values. In comparison to its reference system, the $^{16}O+^{60}Ni$, fusion enhancement is expected in the $^{18}O+^{58}Ni$ system due to the presence of PQNT. Examination of fusion and elastic scattering data of $^{18}O+^{58}Ni$ by Silva *et al.* [83] confirmed the enhancement. Fusion calculations of $^{18}O+^{63,65}Cu$ reactions by Chamon *et al.* [84] do not find any projectile dependence on fusion cross sections. Due to the PQNT channel, it is expected that there would be an enhancement for $^{18}O+^{74}Ge$ in the below-barrier energy region. Their theoretical predictions of fusion data with CC calculation and their barrier distributions show no such effect [80–82]. For $^{18}O+^{92}Mo$ Monteiro *et al.* [86] suggested a need for coupling with transfer channels to explain quasielastic barrier distributions. A comprehensive study on $^{16,18}O+^{112-124}Sn$ by Jacobs *et al.* [39] does not find any enhancement due to the PQNT channel on sub-barrier fusion cross section. Inclusion of PQNT in CC calculations showed an enhancement in $^{18}O+^{116}Sn$ [60].

TABLE III. Lists of ^{18}O induced reactions with their $2n$ stripping Q values, neutron number of target after $2n$ transfer, and target deformations before and after $2n$ stripping.

Reaction	$2n$ stripping Q value	Neutron no. of target after $2n$ transfer	Deformation of target		Expt. evidence for PQNT	Ref.
			Before $2n$ transfer	After $2n$ transfer		
$^{18}O+^{58}Ni \rightarrow {}^{76}Kr$	8.199	32	0.179	0.2050 [87]	Yes	[83]
$^{18}O+^{63}Cu \rightarrow {}^{81}Rb$	5.638	36	0.151	−0.125 [69]	No	[84]
$^{18}O+^{65}Cu \rightarrow {}^{83}Rb$	5.638	38	−0.125	−0.085 [69]	No	[84]
$^{18}O+^{74}Ge \rightarrow {}^{92}Zr$	3.745	44	0.283	0.2623 [68]	No	[80]
$^{18}O+^{92}Mo \rightarrow {}^{110}Sn$	5.559	52	0.1058	0.1509 [68]	Yes	[85,86]
$^{18}O+^{112}Sn \rightarrow {}^{130}Ce$	5.856	64	0.1207	0.1147 [75]	No	[39]
$^{18}O+^{116}Sn \rightarrow {}^{134}Ce$	4.081	68	0.1117	0.1100 [75]	Yes	[60]
$^{18}O+^{118}Sn \rightarrow {}^{136}Ce$	3.400	70	0.1100	0.1063 [75]	No	[39]
$^{18}O+^{124}Sn \rightarrow {}^{142}Ce$	1.735	76	0.0942	0.0825 [75]	No	[39]
$^{18}O+^{150}Sm \rightarrow {}^{168}Yb$	1.666	90	0.1931	0.3065 [68]	Yes	[79]
$^{18}O+^{181}Ta \rightarrow {}^{199}Tl$	0.809	110	0.255	0.244 [75]	No	[72]
$^{18}O+^{182}W \rightarrow {}^{200}Pb$	1.414	110	0.251	0.236 [68]	No	this work
$^{18}O+^{184}W \rightarrow {}^{202}Pb$	0.757	112	0.236	0.226 [68]	No	this work
$^{18}O+^{186}W \rightarrow {}^{204}Pb$	0.113	114	0.226 [68]	0.197 [87]	No	this work

So, in order to conclude the effect of the PQNT channels on fusion enhancement of ^{18}O induced reactions, we looked at the ^{18}O induced reactions that were available in the literature. Compared to the reference systems, cross sections of most of the reactions given in the Table III do not exhibit an enhancement due to the PQNT channel [39,72,80,84]. ^{18}O + ^{58}Ni, ^{18}O + ^{92}Mo, and ^{18}O + ^{150}Sm reactions show an enhancement due to the presence of the PQNT channel [79,83,86]. In these three reactions, after $2n$ transfer, the target deformation increased. As the deformation increases, the barrier height decreases, increasing the below-barrier fusion cross sections. All of this points to the conclusion that, in systems with a PQNT channel, if the system's deformation increases after neutron transfer, it leads to fusion enhancement. Because Z_pZ_t values stay the same after $2n$ transfer, the increase in deformation may lead to the decrease in barrier height, resulting in fusion enhancement. The highlighted systems in Table III, which show an enhancement due to PQNT [79,83,86], reveal that the enhancement occurs only when the deformation of the target increases after $2n$ transfer. Furthermore, a higher $2n$ transfer Q value does not guarantee a more considerable enhancement. Also none of the highlighted systems in Table III approach neutron shell closure values after $2n$ transfer. This confirms that neutron magicity does not have a significant role in fusion enhancement in systems with PQNT channels.

V. SUMMARY AND CONCLUSION

Using a recoil mass spectrometer, we measured the ER excitation function for ^{18}O + ^{182,184,186}W reactions, that populate the compound nuclei ^{200,202,204}Pb respectively. The positive $2n$ transfer Q values of ^{18}O + ^{182,184,186}W reactions predicted an enhancement in the below-barrier energy regions of fusion cross sections. However, no specific signatures of fusion enhancement are found in the positive $2n$ transfer Q value systems ^{18}O + ^{182,184,186}W, in comparison with negative $2n$ transfer Q value systems ^{16}O + ^{182,184,186}W.

To explain the experimental excitation functions of ^{18}O + ^{182,184,186}W, we have analyzed the measured cross sections by including different inelastic excitation channels in the CC calculations. Without adding neutron transfer channels, CC calculations described experimental cross sections of all ^{18}O induced reactions except at higher energy points. The CC calculations yielded similar results when transfer coupling was included. An appreciable role by neutron transfer channel in fusion enhancement of ^{18}O + ^{182,184,186}W reactions was thus eliminated. The absence of below-barrier enhancement due to PQNT effects was again confirmed by a self-consistent method using relative enhancement. Systematics studies on ^{18}O induced reactions in different mass regions indicate that an increase in deformation following neutron transfer enhances the cross sections in reactions with PQNT. To get a clear understanding of the effect of PQNT, more experimental investigations on transfer reactions are needed.

ACKNOWLEDGMENTS

We are grateful to the Pelletron group of IUAC for providing an excellent beam of required pulse width throughout the experiment. We are indebted for the support received from the target and data support laboratories of IUAC. One of the authors (P.J.) would like to thank UGC-BSR, New Delhi, for financial support.

[1] B. B. Back, H. Esbensen, C. L. Jiang, and K. E. Rehm, Rev. Mod. Phys. **86**, 317 (2014).
[2] D. W. Bardayan, J. Phys. G Nucl. Part. Phys. **43**, 043001 (2016).
[3] L. Canto, P. Gomes, R. Donangelo, J. Lubian, and M. Hussein, Phys. Rep. **596**, 1 (2015).
[4] K. Hagino, arXiv:2201.08061.
[5] M. Dasgupta, D. J. Hinde, N. Rowley, and A. M. Stefanini, Annu. Rev. Nucl. Part. Sci. **48**, 401 (1998).
[6] C. Y. Wu, W. V. Oertzen, D. Cline, and M. W. Guidry, Annu. Rev. Nucl. Part. Sci. **40**, 285 (1990).
[7] A. B. Balantekin and N. Takigawa, Rev. Mod. Phys. **70**, 77 (1998).
[8] G. Montagnoli and A. M. Stefanini, Eur. Phys. J. A **53**, 169 (2017).
[9] J. R. Leigh, M. Dasgupta, D. J. Hinde, J. C. Mein, C. R. Morton, R. C. Lemmon, J. P. Lestone, J. O. Newton, H. Timmers, J. X. Wei, and N. Rowley, Phys. Rev. C **52**, 3151 (1995).
[10] J. D. Bierman, P. Chan, J. F. Liang, M. P. Kelly, A. A. Sonzogni, and R. Vandenbosch, Phys. Rev. Lett. **76**, 1587 (1996).
[11] A. M. Stefanini, D. Ackermann, L. Corradi, J. H. He, G. Montagnoli, S. Beghini, F. Scarlassara, and G. F. Segato, Phys. Rev. C **52**, R1727 (1995).
[12] V. Tripathi, L. T. Baby, J. J. Das, P. Sugathan, N. Madhavan, A. K. Sinha, P. V. Madhusudhana Rao, S. K. Hui, R. Singh, and K. Hagino, Phys. Rev. C **65**, 014614 (2001).
[13] A. M. Stefanini, D. Ackermann, L. Corradi, D. R. Napoli, C. Petrache, P. Spolaore, P. Bednarczyk, H. Q. Zhang, S. Beghini, G. Montagnoli, L. Mueller, F. Scarlassara, G. F. Segato, F. Soramel, and N. Rowley, Phys. Rev. Lett. **74**, 864 (1995).
[14] A. M. Stefanini, L. Corradi, A. M. Vinodkumar, Y. Feng, F. Scarlassara, G. Montagnoli, S. Beghini, and M. Bisogno, Phys. Rev. C **62**, 014601 (2000).
[15] V. Denisov, Eur. Phys. J. **7**, 34 (2000).
[16] J. M. B. Shorto, P. R. S. Gomes, J. Lubian, L. F. Canto, and P. Lotti, Phys. Rev. C **81**, 044601 (2010).
[17] V. I. Zagrebaev, Phys. Rev. C **67**, 061601(R) (2003).
[18] J. J. Kolata, A. Roberts, A. M. Howard, D. Shapira, J. F. Liang, C. J. Gross, R. L. Varner, Z. Kohley, A. N. Villano, H. Amro, W. Loveland, and E. Chavez, Phys. Rev. C **85**, 054603 (2012).
[19] M. Trotta, A. M. Stefanini, L. Corradi, A. Gadea, F. Scarlassara, S. Beghini, and G. Montagnoli, Phys. Rev. C **65**, 011601(R) (2001).
[20] R. Broglia, C. Dasso, S. Landowne, and G. Pollarolo, Phys. Lett. B **133**, 34 (1983).
[21] S. Kalkal, S. Mandal, N. Madhavan, A. Jhingan, E. Prasad, R. Sandal, S. Nath, J. Gehlot, R. Garg, G. Mohanto, M. Saxena, S. Goyal, S. Verma, B. R. Behera, S. Kumar, U. D. Pramanik, A. K. Sinha, and R. Singh, Phys. Rev. C **83**, 054607 (2011).
[22] C. S. Palshetkar, S. Thakur, V. Nanal, A. Shrivastava, N. Dokania, V. Singh, V. V. Parkar, P. C. Rout, R. Palit,

R. G. Pillay, S. Bhattacharyya, A. Chatterjee, S. Santra, K. Ramachandran, and N. L. Singh, Phys. Rev. C **89**, 024607 (2014).
[23] N. Rowley, G. Satchler, and P. Stelson, Phys. Lett. B **254**, 25 (1991).
[24] O. A. Capurro, J. E. Testoni, D. Abriola, D. E. DiGregorio, J. O. Fernández Niello, G. V. Martí, A. J. Pacheco, M. R. Spinella, M. Ramírez, C. Balpardo, and M. Ortega, Phys. Rev. C **65**, 064617 (2002).
[25] H. M. Jia, C. J. Lin, F. Yang, X. X. Xu, H. Q. Zhang, Z. H. Liu, Z. D. Wu, L. Yang, N. R. Ma, P. F. Bao, and L. J. Sun, Phys. Rev. C **90**, 031601(R) (2014).
[26] L. T. Baby, V. Tripathi, J. J. Das, P. Sugathan, N. Madhavan, A. K. Sinha, M. C. Radhakrishna, P. V. Madhusudhana Rao, S. K. Hui, and K. Hagino, Phys. Rev. C **62**, 014603 (2000).
[27] H. Timmers, D. Ackermann, S. Beghini, L. Corradi, J. He, G. Montagnoli, F. Scarlassara, A. Stefanini, and N. Rowley, Nucl. Phys. A **633**, 421 (1998).
[28] K. Hagino, N. Rowley, and A. Kruppa, Comput. Phys. Commun. **123**, 143 (1999).
[29] K. Hagino and N. Takigawa, Prog. Theor. Phys. **128**, 1061 (2012).
[30] C. Dasso and S. Landowne, Comput. Phys. Commun. **46**, 187 (1987).
[31] M. Beckerman, M. Salomaa, A. Sperduto, H. Enge, J. Ball, A. DiRienzo, S. Gazes, Y. Chen, J. D. Molitoris, and N.-f. Mao, Phys. Rev. Lett. **45**, 1472 (1980).
[32] R. A. Broglia, C. H. Dasso, S. Landowne, and A. Winther, Phys. Rev. C **27**, 2433 (1983).
[33] H. Esbensen, S. H. Fricke, and S. Landowne, Phys. Rev. C **40**, 2046 (1989).
[34] P. Stelson, Phys. Lett. B **205**, 190 (1988).
[35] H.-J. Hennrich, G. Breitbach, W. Kühn, V. Metag, R. Novotny, D. Habs, and D. Schwalm, Phys. Lett. B **258**, 275 (1991).
[36] A. M. Stefanini, F. Scarlassara, S. Beghini, G. Montagnoli, R. Silvestri, M. Trotta, B. R. Behera, L. Corradi, E. Fioretto, A. Gadea, Y. W. Wu, S. Szilner, H. Q. Zhang, Z. H. Liu, M. Ruan, F. Yang, and N. Rowley, Phys. Rev. C **73**, 034606 (2006).
[37] H. Q. Zhang, C. J. Lin, F. Yang, H. M. Jia, X. X. Xu, Z. D. Wu, F. Jia, S. T. Zhang, Z. H. Liu, A. Richard, and C. Beck, Phys. Rev. C **82**, 054609 (2010).
[38] Khushboo, N. Madhavan, S. Nath, A. Jhingan, J. Gehlot, B. Behera, S. Verma, S. Kalkal, and S. Mandal, Phys. Rev. C **100**, 064612 (2019).
[39] P. Jacobs, Z. Fraenkel, G. Mamane, and I. Tserruya, Phys. Lett. B **175**, 271 (1986).
[40] Z. Kohley, J. F. Liang, D. Shapira, R. L. Varner, C. J. Gross, J. M. Allmond, A. L. Caraley, E. A. Coello, F. Favela, K. Lagergren, and P. E. Mueller, Phys. Rev. Lett. **107**, 202701 (2011).
[41] A. M. Stefanini, G. Montagnoli, F. Scarlassara, C. L. Jiang, H. Esbensen, E. Fioretto, L. Corradi, B. B. Back, C. M. Deibel, B. Di Giovine, J. P. Greene, H. D. Henderson, S. T. Marley, M. Notani, N. Patel, K. E. Rehm, D. Sewerinyak, X. D. Tang, C. Ugalde, and S. Zhu, Eur. Phys. J. A **49**, 034606 (2013).
[42] C. J. Lin, H. M. Jia, H. Q. Zhang, X. X. Xu, F. Yang, L. Yang, P. F. Bao, L. J. Sun, and Z. H. Liu, EPJ Web Conf. **66**, 03055 (2014).
[43] C. L. Jiang, K. E. Rehm, B. B. Back, H. Esbensen, R. V. F. Janssens, A. M. Stefanini, and G. Montagnoli, Phys. Rev. C **89**, 051603(R) (2014).
[44] V. A. Rachkov, A. V. Karpov, A. S. Denikin, and V. I. Zagrebaev, Phys. Rev. C **90**, 014614 (2014).
[45] G. L. Zhang, X. X. Liu, and C. J. Lin, Phys. Rev. C **89**, 054602 (2014).
[46] A. A. Ogloblin, H. Q. Zhang, C. J. Lin, H. M. Jia, S. V. Khlebnikov, E. A. Kuzmin, W. H. Trzaska, X. X. Xu, F. Yan, V. V. Sargsyan, G. G. Adamian, N. V. Antonenko, and W. Scheid, Eur. Phys. J. A **50**, 157 (2014).
[47] V. V. Sargsyan, G. G. Adamian, N. V. Antonenko, W. Scheid, and H. Q. Zhang, Phys. Rev. C **84**, 064614 (2011).
[48] V. V. Sargsyan, G. G. Adamian, N. V. Antonenko, W. Scheid, and H. Q. Zhang, Phys. Rev. C **85**, 024616 (2012).
[49] M. Dasgupta, P. R. S. Gomes, D. J. Hinde, S. B. Moraes, R. M. Anjos, A. C. Berriman, R. D. Butt, N. Carlin, J. Lubian, C. R. Morton, J. O. Newton, and A. Szanto de Toledo, Phys. Rev. C **70**, 024606 (2004).
[50] K. Hagino, A. Vitturi, C. H. Dasso, and S. M. Lenzi, Phys. Rev. C **61**, 037602 (2000).
[51] L. Canto, P. Gomes, J. Lubian, L. Chamon, and E. Crema, Nucl. Phys. A **821**, 51 (2009).
[52] V. A. Rachkov, A. Adel, A. V. Karpov, A. S. Denikin, V. I. Zagrebaev, P. A. DeYoung, G. F. Peaslee, B. Hughey, B. Atalla, M. Kern, P. L. Jolivette, J. A. Zimmerman, M. Y. Lee, F. D. Becchetti, E. F. Aguilera, E. Martinez-Quiroz, and J. D. Hinnefeld, Bull. Russ. Acad. Sci.: Phys. **77**, 411 (2013).
[53] V. I. Zagrebaev, V. V. Samarin, and W. Greiner, Phys. Rev. C **75**, 035809 (2007).
[54] N. Rowley, I. Thompson, and M. Nagarajan, Phys. Lett. B **282**, 276 (1992).
[55] C. A. Bertulani, EPJ Web Conf. **17**, 15001 (2011).
[56] J. R. Leigh, J. J. M. Bokhorst, D. J. Hinde, and J. O. Newton, J. Phys. G Nucl. Part Phys. **14**, L55 (1988).
[57] M. Trotta, A. M. Stefanini, S. Beghini, B. R. Behera, A. Yu. Chizhov, L.Corradi, S. Courtin, E. Fioretto, A. Gadea, P. R. S. Gomes, F. Haas, I. M. Itkis, M. G. Itkis, G. N. Kniajeva, N. A. Kondratiev, E. M. Kozulin, A. Latina, G. Montagnoli, T. V. Pokrovsky, N. Rowley *et al.*, Eur. Phys. J. A **25**, 615 (2005).
[58] D. J. Hinde, W. Pan, A. C. Berriman, R. D. Butt, M. Dasgupta, C. R. Morton, and J. O. Newton, Phys. Rev. C **62**, 024615 (2000).
[59] V. V. Sargsyan, G. G. Adamian, N. V. Antonenko, W. Scheid, and H. Q. Zhang, Phys. Rev. C **86**, 014602 (2012).
[60] N. K. Deb, K. Kalita, H. A. Rashid, S. Nath, J. Gehlot, N. Madhavan, R. Biswas, R. N. Sahoo, P. K. Giri, A. Das, T. Rajbongshi, A. Parihari, N. K. Rai, S. Biswas, Khushboo, A. Mahato, B. J. Roy, A. Vinayak, and A. Rani, Phys. Rev. C **102**, 034603 (2020).
[61] A. Sinha, N. Madhavan, J. Das, P. Sugathan, D. Kataria, A. Patro, and G. Mehta, Nucl. Instrum. Methods Phys. Res., Sect. A **339**, 543 (1994).
[62] E. T. Subramaniam, B. P. Ajith Kumar, and R. K. Bhowmik, Candle – collection and analysis of nuclear data using linux network (unpublished).
[63] S. Nath, Comput. Phys. Commun. **180**, 2392 (2009).
[64] S. Nath, Comput. Phys. Commun. **181**, 1659 (2010).
[65] A. Gavron, Phys. Rev. C **21**, 230 (1980).
[66] J. Gehlot, S. Nath, T. Banerjee, I. Mukul, R. Dubey, A. Shamlath, P. V. Laveen, M. Shareef, M. M. Shaikh, A. Jhingan, N. Madhavan, T. Rajbongshi, P. Jisha, and S. Pal, Phys. Rev. C **99**, 061601(R) (2019).

[67] CCFULL (a version with two different modes of excitation both in the projectile and in the target), http://www2.yukawa.kyoto-u.ac.jp/~kouichi.hagino/ccfull.html.
[68] S. Ramen, C. W. Nestor, and P. Tikkanen, At. Data Nucl. Data Tables **78**, 1 (2001).
[69] P. Möller, A. J. Sierk, T. Ichikawa, and H. Sagawa, At. Data Nucl. Data Tables **109-110**, 1 (2016).
[70] R. Lemmon, J. Leigh, J. Wei, C. Morton, D. Hinde, J. Newton, J. Mein, M. Dasgupta, and N. Rowley, Phys. Lett. B **316**, 32 (1993).
[71] C. E. Bemis Jr., T. C. Awes, J. R. Beene, R. L. Ferguson, H. Kim, F. K. McGowan, F. Obenshain, F. E.and Plasil, Z. Jacobs, P.and Frankel, U. Smilansky, and I. Tserruya, ORNL Progress Report, 1986 (unpublished).
[72] P. Jisha, A. M. Vinodkumar, B. R. S. Babu, S. Nath, N. Madhavan, J. Gehlot, A. Jhingan, T. Banerjee, I. Mukul, R. Dubey, N. Saneesh, K. M. Varier, E. Prasad, A. Shamlath, P. V. Laveen, and M. Shareef, Phys. Rev. C **101**, 024611 (2020).
[73] T. Kibedi and R. Spear, At. Data Nucl. Data Tables **80**, 35 (2002).
[74] K. Hagino, N. Takigawa, M. Dasgupta, D. J. Hinde, and J. R. Leigh, Phys. Rev. Lett. **79**, 2014 (1997).
[75] V. I. Zagrebaev, A. S. Denikin, A. V. Karpov, A. P. Alekseev, M. A. Naumenko, V. A. Rachkov, V. V. Samarin, and V. V. Saiko, NRV web knowledge base on low-energy nuclear physics (1999).
[76] S. Saha, Y. K. Agarwal, and C. V. K. Baba, Phys. Rev. C **49**, 2578 (1994).
[77] C. Dasso and G. Pollarolo, Phys. Lett. B **155**, 223 (1985).
[78] M. Firihu, K. Hagino, and N. Takigawa, in *FUSION06: Reaction Mechanisms and Nuclear Structure at the Coulomb Barrier, 19–23 March 2006, San Servolo, Venezia, Italy*, edited by L. Corradi, D. Ackermann, E. Fioretto, A. Gadea, F. Haas, G. Pollarolo, F. Scarlassara, S. Szilner, and M. Trotta, AIP Conf. Proc. No. 853 (AIP, New York, 2006).
[79] R. Charity, J. Leigh, J. Bokhorst, A. Chatterjee, G. Foote, D. Hinde, J. Newton, S. Ogaza, and D. Ward, Nucl. Phys. A **457**, 441 (1986).
[80] H. M. Jia, C. J. Lin, F. Yang, X. X. Xu, H. Q. Zhang, Z. H. Liu, L. Yang, S. T. Zhang, P. F. Bao, and L. J. Sun, Phys. Rev. C **86**, 044621 (2012).
[81] H. Jia, C. Lin, F. Yang, X. xu, H. Zhang, Z. Liu, L. Yang, S. Zhang, P. Bao, and L.-J. Sun, J. Phys.: Conf. Ser. **420**, 2124 (2013).
[82] C. J. Lin, H. M. Jia, H. Q. Zhang, X. X. Xu, X. F. Yang, X. L. Yang, P. F. Bao, L. J. Sun, and Z. H. Liu, EPJ Web Conf. **63**, 02007 (2013).
[83] C. P. Silva, D. Pereira, L. C. Chamon, E. S. Rossi, G. Ramirez, A. M. Borges, and C. E. Aguiar, Phys. Rev. C **55**, 3155 (1997).
[84] L. C. Chamon, D. Pereira, E. S. Rossi, C. P. Silva, G. R. Razeto, A. M. Borges, L. C. Gomes, and O. Sala, Phys. Lett. B **275**, 29 (1992).
[85] M. Benjelloun, W. Galster, and J. Vervier, Nucl. Phys. A **560**, 715 (1993).
[86] D. Monteiro, R. Simões, J. Shorto, A. Jacob, L. Ono, L. Paulucci, N. Added, and E. Crema, Nucl. Phys. A **725**, 60 (2003).
[87] National Nuclear Data Center, Brookhaven National Laboratory, 2008, https://www.nndc.bnl.gov/nudat2.